

## Production of Strange Particles by $\pi^- - p$ Interactions near Threshold\*

L. B. LEIPUNER AND R. K. ADAIR  
*Brookhaven National Laboratory, Upton, New York*  
 (Received October 11, 1957)

Observations have been made, in a liquid hydrogen bubble chamber, of the production and decay of strange particles produced by the interaction of 960-Mev  $\pi^-$  mesons with protons. The total strange particle production cross section was measured to be  $1.02 \pm 0.20$  millibarns. The cross section is  $0.58 \pm 0.12$  millibarn for  $\Lambda^0 - \theta^0$  production,  $0.35 \pm 0.09$  millibarn for  $\Sigma^0 - K^+$  production, and is  $0.09 \pm 0.04$  millibarn for  $\Sigma^- - K^+$  particles. Production angular distribution was peaked somewhat backwards for  $\Sigma^0$  and  $\Lambda^0$  hyperons. These cross sections, together with other data, are interpreted as indicating the existence of a very strong interaction for the production of strange particles which extends over a small radius. The decay products of the  $\Lambda^0$  hyperons from  $\Lambda^0 - \theta^0$  production were preferentially aligned with the incoming beam, a result suggesting a spin of  $\frac{3}{2}$  for the  $\Lambda^0$ . Decay distributions for  $\Lambda^0$  particles resulting from  $\Sigma^0$  decay, and for  $\theta^0$  mesons, were consistent with isotropy.

### I. INTRODUCTION

EARLY measurements by the Brookhaven cloud chamber group<sup>1</sup> established a cross section of about one millibarn for the production of strange particles by the interaction of 1.4-Bev  $\pi^-$  mesons with protons. Although the number of events recorded was small, both charged and neutral  $\Sigma$  hyperons were observed, and the results suggested that  $\Lambda^0$  hyperons were produced preferentially backwards while  $\Sigma^-$  particles were produced preferentially in the forward direction. These conclusions were greatly strengthened by the observations of Budde *et al.*<sup>2</sup> using a propane bubble chamber to observe interactions at 1.3 Bev. Walker and Shephard<sup>3</sup> have shown, on the basis of five events observed in a diffusion cloud chamber, that the  $\pi^- - p$  strange particle production cross section is also about a millibarn at 950 Mev.

It has been the experience in large areas of nuclear physics that the dynamics of reactions is most easily interpretable at energies near threshold where only states with zero or one unit of orbital angular momentum are important. In particular the spins of the strange particles might be obtained from the angular distribution of their decay products.<sup>4,5</sup>

For these reasons it appeared especially desirable to examine the production cross sections, angular distributions, and decay distributions near threshold. The threshold for the production of  $\Lambda^0$  hyperons by the  $\pi^- - p$  reaction is about 760 Mev  $\pi^-$  kinetic energy in the laboratory system and about 900 Mev for  $\Sigma - K$  production. We chose to investigate these reactions at a  $\pi^-$  energy of 960 Mev. At this energy the center-of-

mass momentum of the  $\Lambda^0 - \theta^0$  is about 280 Mev/ $c$ , and the  $\Sigma - K$  momentum is about 140 Mev/ $c$ . Since these values are small compared to  $\hbar$  divided by a plausible complimentary length  $\hbar/M_K c$ , where  $M_K$  is the mass of the  $K$  meson, it seemed reasonable to assume that most of the production intensity results from  $S$  or  $P$  states of orbital angular momentum.

### II. EQUIPMENT

A liquid hydrogen bubble chamber 6 inches long, 3 inches wide, and 2 inches deep, was constructed and used in these measurements. This chamber differs in some fundamental respects from previous liquid hydrogen chambers.<sup>6,7</sup> In particular, the liquid hydrogen in the chamber is expanded and compressed by the motion of a piston which acts directly on the liquid, and the temperature of the chamber is determined, and controlled, by controlling the pressure at which liquid hydrogen in a reservoir is allowed to evaporate. This reservoir is closely coupled thermally to the chamber. No extraneous controlling heat is introduced.

A schematic view of the chamber is shown in Fig. 1. The body of the chamber was machined from a forged block of electrolytic copper. Glass windows,  $\frac{3}{4}$  of an inch thick, are held in place with stainless steel flanges. The glass-to-metal seal at each window is effected by two indium wire gaskets. Differential pumping is applied between the two gaskets. Usually the inside gasket is tight, at least to the extent that any existing leak is smaller than our normal observable limit of about  $2 \times 10^{-6}$  liters S.T.P./second of hydrogen.

The aluminum piston, fitted with four automobile type piston rings made of Textolite, acts as a high impedance to the hydrogen rather than a tight barrier. A test of the piston at room temperature showed that about 100 cm<sup>3</sup> S.T.P./sec of nitrogen gas would pass the piston rings when a pressure of 100 psi gauge was applied to one side.

\* Work performed under the auspices of the U. S. Atomic Energy Commission.

<sup>1</sup> Fowler, Shutt, Thorndike, and Whittemore, Phys. Rev. **91**, 1287 (1953); **93**, 861 (1954).

<sup>2</sup> Budde, Chretien, Leitner, Samios, Schwartz, and Steinberger, Phys. Rev. **103**, 1827 (1956).

<sup>3</sup> W. D. Walker and W. D. Shephard, Phys. Rev. **101**, 1810 (1956).

<sup>4</sup> M. I. Shirokov, J. Exptl. Theoret. Phys. U.S.S.R. **31**, 734 (1956) [translation: Soviet Phys. JETP **4**, 620 (1957)].

<sup>5</sup> Robert K. Adair, Phys. Rev. **100**, 1540 (1955).

<sup>6</sup> Douglas Parmentier, Jr., and Arnold J. Schwemin, Rev. Sci. Instr. **26**, 954 (1956).

<sup>7</sup> Nagle, Hildebrand, and Plano, Rev. Sci. Instr. **27**, 203 (1956).

In operation the chamber is surrounded by a copper radiation shield held at liquid nitrogen temperature. Both chamber and radiation shield are contained in an evacuated can. The chamber is illuminated and photographed through glass windows in the vacuum jacket. Since the heat shield is cut away for illumination and photography, the faces of the chamber are exposed to 300°K radiation over a large angular aperture. Most of the heat input to the chamber, which leads to a quiescent or Dewar loss of about one liter of hydrogen per hour, is the result of this radiation. Little increase has been noted in the hydrogen evaporation rate when the chamber was operated at the rate of once every three seconds. In general the hydrogen consumption is moderate. Approximately thirty liters of hydrogen is sufficient to cool the chamber from liquid nitrogen temperature to hydrogen temperature, to fill the chamber, and to fill the reservoirs with sufficient hydrogen for a twelve-hour run.

During operation the chamber is held at a temperature,  $T_c$ , which may vary from 27° to 29° depending upon the bubble density desired. This temperature is held constant to about  $\pm 0.04^\circ$  by controlling the pressure, and hence the temperature, of the reservoir by means of a manostat. This reservoir is connected to the body of the chamber through heavy copper bars which keep the temperature differential between the reservoir and the chamber to about 0.15°K. This chamber temperature is measured by a hydrogen vapor pressure thermometer, which uses a hole drilled into the chamber body as its bulb.

The chamber is filled by condensing hydrogen gas in a heat exchanger cooled by liquid hydrogen in the reservoir. This condensed hydrogen leaks past the piston rings into the chamber. A pressure about 10 psi greater than the reading of the chamber vapor pressure thermometer is applied to the hydrogen in the chamber through the filling line. This results in hydrogen condensing above the piston to a level in the piston enclosure determined by the temperature gradient in effect.

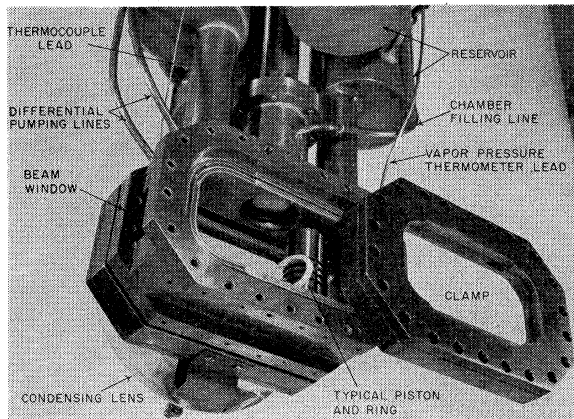


FIG. 1. Schematic view of liquid hydrogen bubble chamber.

An air-driven piston acts through a stainless steel rod to move the chamber piston up and down during operation. Pressure in the chamber was measured by a transducer which consisted of a parallel plate condenser, one plate of which was a thin steel diaphragm soldered into the chamber. A change in capacitance approximately proportional to the pressure change was easily measured. The change in chamber volume is about 1.5%. Knowledge of the volume change and pressure change has the incidental advantage of enabling us to know the density of the hydrogen in the active chamber with an error of about 1%. For the majority of the measurements made in this experiment the temperature was held at 28.35° and the density of the expanded hydrogen was then about 1.2% less than the density of 0.0560 g/cc measured at the pressure corresponding to the vapor pressure at this temperature. This density depends upon ortho-para concentration and the largest error in our knowledge of the density is due to the uncertainty in the parahydrogen concentration.

A stereoscopic camera with an interocular of  $3\frac{1}{4}$  inches photographs the chamber from a distance of about 12 inches. A condensing lens mounted on the chamber focuses an image of an extended light source to an area between the lenses of the camera. The effect of the severe reflections often observed in small-angle dark-field photography is reduced by using an extended source. The first associated  $\Lambda^0-\theta^0$  observed in this experiment is shown in Fig. 2. This picture was taken three milliseconds after the beam passed through the chamber. The turbulence evident beneath the piston probably results from poor hydrodynamic design of the chamber. This turbulence results in distortion of tracks which pass very near the top of the chamber. Only very slight distortion occurs in tracks which are an inch or more from the top of the chamber. A deviation of about 100  $\mu$  upward is noticed in the center of tracks passing through the chamber, equivalent to a radius of curvature of about 25 meters. Besides these distortions occasional local distortions are noted which also result in displacements of the order of 100  $\mu$ . These disturbances take place over volumes of the order of 0.1 cm<sup>3</sup> and do not appear to be reproduced from picture to picture.

### III. PROCEDURE AND RESULTS

A beam of 960-Mev  $\pi^-$  mesons was produced by bombarding a beryllium target, situated in a Cosmotron straight section, with 2-Bev protons. Mesons produced in the forward direction passed into the Cosmotron field and the negative mesons were bent out of the vacuum chamber through a thin window. Though the primary momentum analysis was provided by the Cosmotron field, the particles were bent again about 25° into the chamber by the field of a deflecting magnet. The  $\pi^-$  kinetic energy was 960 Mev as calculated from the magnetic field of the cosmotron and the constraints of the orbit. A largely independent measurement was

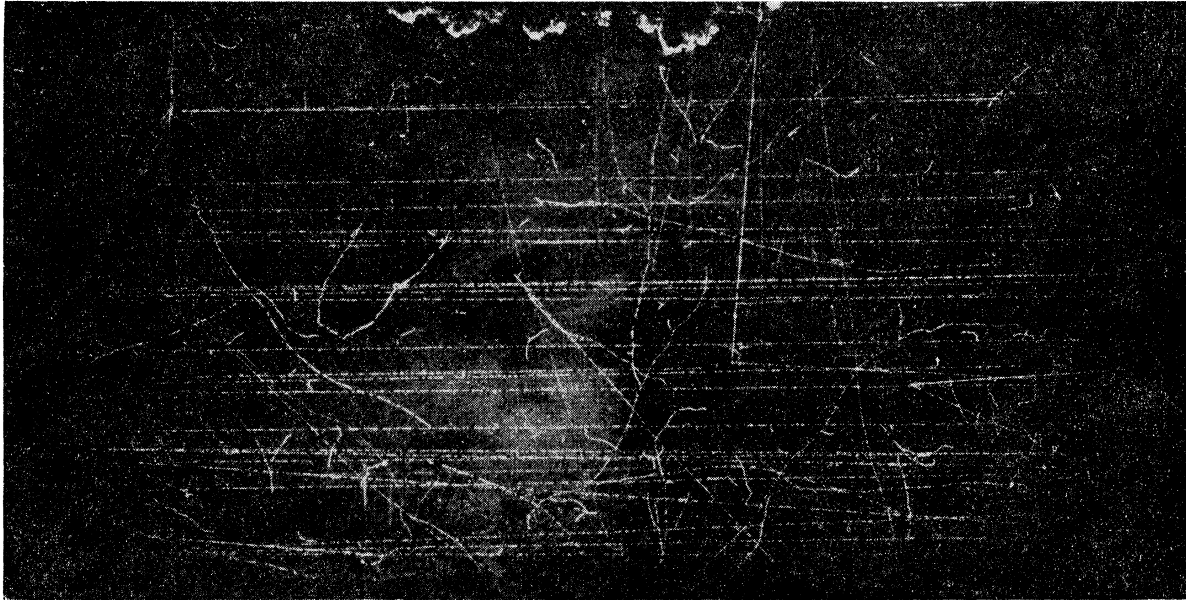


FIG. 2. A  $\pi^- + p \rightarrow \Lambda^0 + \theta^0$  event observed in the bubble chamber.

made by determining the force on a current-carrying wire which passed through the field of the deflecting magnet. The energy spread indicated by the calculations and by the measurements, was  $\pm 10$  Mev. The primary proton current was adjusted so a  $\pi^-$  meson flux of about  $0.5/\text{cm}^2$  pulse was incident upon the chamber at a repetition rate of once every three and one-half seconds. This allowed about 13 tracks per pulse through the three square inches of chamber window.

The pictures were projected to a size four times that of the chamber for scanning and measuring. Results of the measurements were recorded on punched cards which were used as the input data for a digital computer. The computer was used to calculate the positions of all tracks in space, distances between pertinent points, and angles between lines and lines, lines and planes, and planes and planes. Events were identified and classified by comparing the angles of production and decay of the particles, with angles read from tables of kinematics computed by the use of the same machine.

Since only two-body reactions were considered in this work, knowledge of the production and decay angles is generally sufficient to allow identification of the type of event to determine the angles of production and decay in the center-of-mass system. In a few cases, it was necessary to consider qualitatively the bubble density of a track to distinguish between the possibility that a track was produced by a relatively slow proton or by a relativistic meson. Another type of identification which required careful consideration was the differentiation between a  $\Lambda^0$  produced directly in  $\Lambda^0-\theta^0$  production and a  $\Lambda^0$  which resulted from the decay of a  $\Sigma^0$ , produced in a  $\Sigma^0-\theta^0$  production. If the  $\theta^0$  is observed, the identification depends on the  $\theta^0$  production

and decay angles and is simple and precise. However, in a majority of cases the  $\theta^0$  does not materialize in the chamber. Identification is, however, still possible. Since the incident  $\pi^-$  energy is very near the  $\Sigma-K$  threshold, the  $\Sigma^0$  is produced at small angles in the laboratory system with velocities which do not differ greatly from the velocity of the center-of-mass. When the  $\Sigma^0$  decays it emits a  $\Lambda^0$  with a momentum<sup>8</sup> of about  $70 \text{ Mev}/c$  in the  $\Sigma^0$  rest system. This impulse is not sufficient to project the  $\Lambda^0$  into the angle *vs* momentum relationships, characteristic of  $\Lambda^0-\theta^0$  production. In almost all cases the accuracy of the measurement was sufficient to distinguish between the two possibilities.

Near threshold the kinematic relationships between laboratory angles of production and decay are quite sensitive to the energy of the incident particle. For most  $\Sigma^- - K^+$  events and for most  $\Sigma^0 - \theta^0$  events in which the  $\theta^0$  is observed, the incoming particle energy can be accurately calculated. Examination of these events indicates the mean energy of the incoming beam was  $960 \pm 5$  Mev, with a spread of  $\pm 10$  Mev. This result is consistent with the wire measurements.

Some 53 strange particle events have been observed, of which 6 were identified as  $\Sigma^- - K^+$  events, 18 as  $\Sigma^0 - \theta^0$  events, and 28 as  $\Lambda^0 - \theta^0$  events. One apparent  $\theta_2$  was seen. In order to establish relative cross sections it is necessary to correct the raw numbers by a factor proportional to the probability that the particles decayed by a neutral or very long-lived mode, and by the probability that the particle left the chamber before decaying. We have taken the value of 0.65 for the portion of  $\Lambda^0$  which decay by charged modes,<sup>7</sup> and 0.45

<sup>8</sup> Plano, Samios, Schwartz, and Steinberger, *Nuovo cimento* **5**, 217 (1957).

for the proportion of  $\theta^0$  mesons which decay by short-lived charged modes.<sup>9</sup> These numbers must be corrected for our estimate of the probability that the short-lived charged decay mode leaves the chamber before decaying or materializing. These considerations lead to the conclusion that we see about 55% of  $\Lambda^0-\theta^0$  or  $\Sigma^0-\theta^0$  production events and about 76% of  $\Sigma^- - K^+$  events. These numbers would be about 67% and 88%, respectively, for a chamber twice as large in each dimension.

Ordinarily the incident flux is measured by counting the number of tracks traversing the chamber. A correction must be made for  $\mu$  mesons and electrons which contaminate the beam. Previous measurement with counters<sup>10</sup> on similar beams indicated that we might expect about 8%  $\mu$  mesons and about 2% electrons. A counter measures a shower of electrons as a single count while a chamber may record several tracks. Since more collimation was used in our measurements than in the counter measurements, it seemed likely to us that our contamination of electrons might be increased by shower production in our collimators and that a count of tracks in the beam would not prove a reliable measure of the  $\pi^-$  flux.

Therefore we used the measured  $\pi^- - p$  cross section<sup>10</sup> at 960 Mev as a standard. Erwin and Kopp<sup>11</sup> scanned a portion of our film with great care, and located and measured about 1200  $\pi^- - p$  interactions. These included stops or zero-prong events, and 17 strange-particle production events. Throughout the measure-

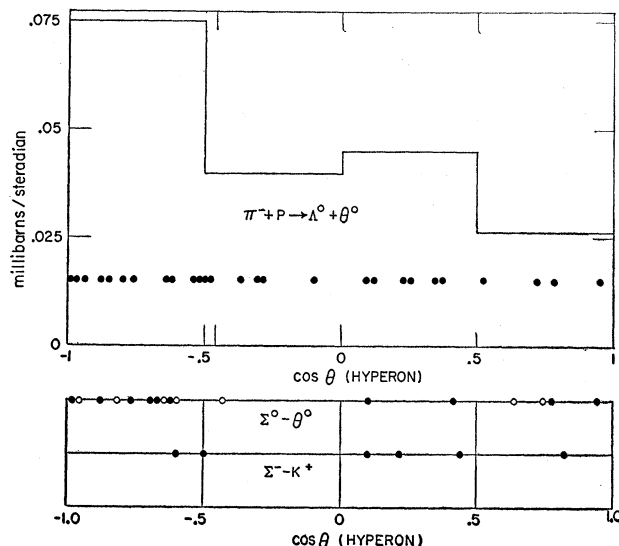


FIG. 3. Strange-particle production angular distribution in the center-of-mass system. Each circle indicates one event. The open circles on the  $\Sigma^0-\theta^0$  graph represent events where a  $\theta^0$  is observed and measured, the solid circles represent events in which only the  $\Lambda^0$  is observed. The angular resolution for  $\Sigma^0$  events in which only the  $\Lambda^0$  is observed is poor.

<sup>9</sup> Eisler, Plano, Samios, Schwartz, and Steinberger, Nuovo cimento **5**, 1700 (1957).

<sup>10</sup> Cool, Piccioni, and Clark, Phys. Rev. **103**, 1082 (1956).

<sup>11</sup> A. Erwin and J. Kopp, Phys. Rev. **109**, 1364 (1958), following paper.

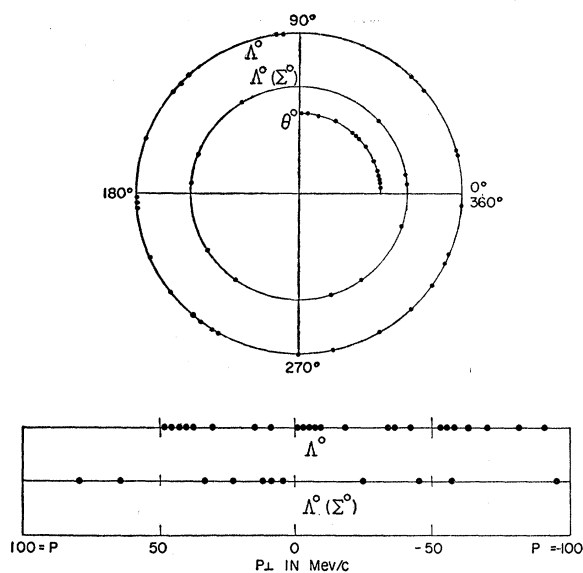


FIG. 4. Decay distributions of  $\Lambda^0$  and  $\theta^0$  particles with respect to the production plane. The polar graph shows the distribution of the angles between planes of production and decay for  $\theta^0$  mesons, for  $\Lambda^0$  hyperons produced directly and for  $\Lambda^0$  hyperons resulting from the decay of  $\Sigma^0$  particles, noted as  $\Lambda^0(\Sigma^0)$ . For hyperons the direction of the production plane is taken as the direction of the vector product  $\mathbf{P}(\pi) \times \mathbf{P}(\Lambda^0)$ , while the direction of the decay plane is the direction  $\mathbf{P}(p) \times \mathbf{P}(\Lambda^0)$ . The sign of the angle is taken to be the sign of the quantity  $[\mathbf{P}(\pi) \times \mathbf{P}(\Lambda^0)] \times [\mathbf{P}(p) \times \mathbf{P}(\Lambda^0)]$ , where  $P$  represents the vector momentum of the particles. The linear plot shows the component of momentum of the decay proton from the  $\Lambda^0$  in the direction of  $\mathbf{P}(\pi) \times \mathbf{P}(\Lambda^0)$ .

ment 3500  $\pi$ -meson interactions were noted together with 51 strange particles. This leads to the following production cross sections:  $\sigma(\Sigma^- - K^+) = 0.09 \pm 0.04$  millibarn,  $\sigma(\Sigma^0 - \theta^0) = 0.35 \pm 0.09$  millibarn,  $\sigma(\Lambda^0 - \theta^0) = 0.58 \pm 0.12$  millibarn, and a total strange-particle production cross section of  $1.02 \pm 0.20$  millibarns.

Angular distributions deduced from the data are shown in Fig. 3. Since the probability of a particle escaping the chamber is dependent on the angle at which it is produced, differential corrections, nowhere larger than 20%, have been applied to the data. The planes of decay of the strange particles relative to the plane of production are shown in Fig. 4. Decay planes for  $\theta^0$  decay, and for  $\Lambda^0$  produced by  $\Sigma^0$  decay, are isotropically distributed while the  $\Lambda^0$  produced directly show a tendency to decay in the lower hemisphere as defined in the caption of Fig. 4. This tendency of the  $\Lambda^0$  decay is shown in a more pertinent manner in Fig. 4 by the distribution in values of the decay proton's component of momentum perpendicular to the production plane.

Decay angular distributions of the strange particles are shown in Fig. 5. The decay with respect to the direction of the incoming beam, rather than the direction of production, is plotted. Again the  $\theta^0$  mesons and the  $\Lambda^0$  from  $\Sigma^0$  decay appear to decay isotropically while the  $\Lambda^0$  produced directly decay preferentially in the direction of the beam. The angular distributions

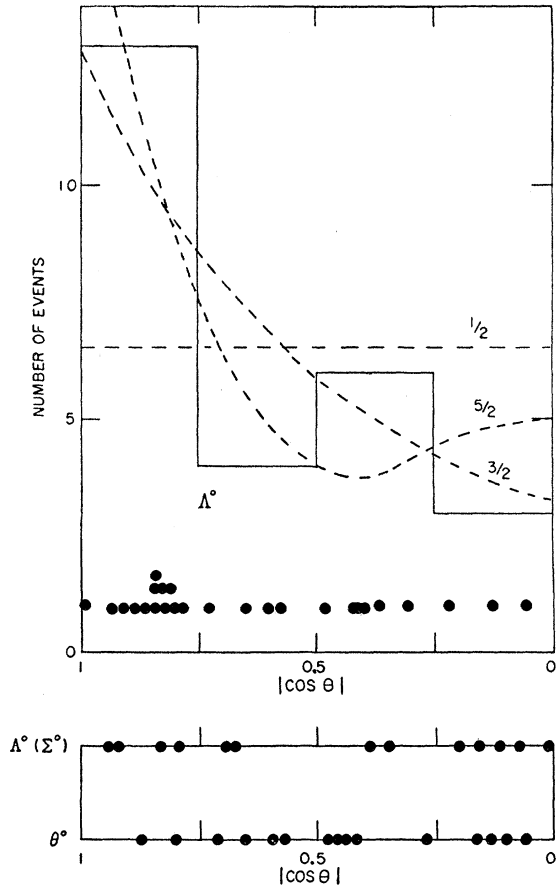


FIG. 5. Decay angular distributions of strange particles. The angle plotted is the angle between the direction of decay of the strange particle and the direction of the incoming beam, observed in the center-of-mass system of the strange particle. The notation  $\Lambda^0(\Sigma^0)$  refers to  $\Lambda^0$  produced from  $\Sigma^0$  decays. The dashed curves on the  $\Lambda^0$  decay histogram represent distributions to be expected for various spins of the  $\Lambda^0$ .

with respect to the production direction are not shown but look rather similar to those of Fig. 4. The forward-to-backward ratio is about one for all processes.

#### IV. CONCLUSIONS

Since the relative momentum of the strange particles produced at 960 Mev is small, it seems likely that most of the production intensity is due to the production of the particles with zero units of orbital angular momentum. Near threshold, the variation of a cross section is predominantly determined by the angular momentum,  $L$ , of the resultant products,<sup>12</sup> and the cross section will increase as  $p^{2L+1}$  where  $p$  is the center-of-mass momentum of the particles which are produced. The existence of the large cross section of one millibarn just above threshold for  $\Lambda^0$  and  $\Sigma$  hyperons, together with the result of Fowler *et al.*<sup>1</sup> that the strange particle production cross section at 1.4 Bev is also about one millibarn,

<sup>12</sup> E. P. Wigner, Phys. Rev. **73**, 1002 (1948).

illustrates a variation of cross section with energy that strongly indicates that  $S$ -wave interaction is dominant at 960 Mev. The anisotropy of the  $\Lambda^0$  production is not at all inconsistent with this conclusion, as a  $P$ -wave contribution of 5% in intensity can account for such distributions.

If the  $P$ -wave intensity is small the arguments of reference 4 hold for production at all angles and it should be possible to derive some information concerning the spins of the  $\theta^0$  and the  $\Lambda^0$ . In particular, if the spin of the  $\theta^0$  is zero the angular distribution of the  $\Lambda^0$  decay with respect to the incoming beam depends uniquely upon the spin of the  $\Lambda^0$ . The dotted curves in Fig. 5 show the distributions in the c.m. system expected for various spins. The measured distribution favors spin  $\frac{3}{2}$  or  $\frac{5}{2}$  over spin  $\frac{1}{2}$ . The likelihood function defined as  $\prod f_{\frac{3}{2}}(\Theta)/f_{\frac{1}{2}}(\Theta)$  where  $f_{\frac{3}{2}}=1$ ,  $f_{\frac{1}{2}}=\frac{1}{2}+\frac{3}{2}\cos^2\Theta$  ( $\Theta$  being the angle of decay of the  $\Lambda^0$  in the c.m. system), and the product is taken for all events, favor spin  $\frac{3}{2}$  over spin  $\frac{1}{2}$  by about 25:1. Spin  $\frac{5}{2}$  and higher spins are less strongly favored. There is other evidence,<sup>13,14</sup> of at least equal validity, which indicated that the spin of the  $\Lambda^0$  is  $\frac{1}{2}$ . If we accept the value of  $\frac{1}{2}$ , assuming for the moment that the present spin results are the result of a statistical fluctuation, we can make some statements concerning the spin of the  $\theta^0$ . The Dalitz analysis of  $\tau$ -meson decays shows that the  $K$  meson can have spin 0 or 2. If the spin is 2 and the spins of the  $\Lambda^0$  and  $\Sigma^0$  are  $\frac{1}{2}$ , the decay distribution of the  $\theta^0$  will take the form  $\alpha(\Theta_2^0)^2+(1-\alpha)(\Theta_2^1)^2$ , where  $0\leq\alpha\leq 1$  and  $\Theta_n^m$  is a spherical harmonic. The decay will, of course, be isotropic if the spin is zero. The likelihood  $\prod[\alpha(\Theta_2^0)^2+(1-\alpha)(\Theta_2^1)^2]/(\Theta_0^0)^2$  was calculated as a function of  $\alpha$ , and it was found that spin 2 was only 6% as probable as spin 0, for the most favorable value of  $\alpha$ ,  $\alpha=0.4$ , and had negligible probability for values of  $\alpha$  which are much different. This conclusion, that the spin is very likely 0, is invalid if the hyperon spin is  $\frac{3}{2}$ .

Lee *et al.*<sup>15</sup> have pointed out that the hyperons might decay preferentially up, or down, with respect to the production plane if parity is not conserved in the decay process. If the spin of the  $\Lambda^0$  is  $\frac{1}{2}$ , the distribution of the components of momentum of the decay proton perpendicular to the production plane will be proportional to  $1+a(P/P_{\max})$ , where  $a$  can be regarded as the product of the polarization of the  $\Lambda^0$  and the proportion of  $\Lambda^0$  which decay without conserving parity. The distribution of Fig. 4 would best represent an  $a$  of about  $-0.5$ , but is only about two probable errors from  $a=0$ . If the spin of the  $\Lambda^0$  is  $\frac{3}{2}$ , the analysis is more complex;

<sup>13</sup> Malvin Ruderman and Robert Karplus, Phys. Rev. **102**, 247 (1954).

<sup>14</sup> G. Puppi *et al.*, *Proceedings of the Seventh Annual Rochester Conference on High-Energy Nuclear Physics, 1957* (Interscience Publishers, Inc., New York, 1957).

<sup>15</sup> Lee, Steinberger, Feinberg, Kabir, and Yang, Phys. Rev. **106**, 1367 (1957).

however, these data still indicate nonconservation of parity with equal strength, or better, weakness.

If we again assume that the spin of the hyperons is one-half and that the  $K$  spin is zero, we see that the measured cross section of one millibarn is an appreciable fraction of the total possible for absorption processes which lead to states of a definite parity and a total angular momentum of one-half. This is equal to  $\pi k^{-2}$  or 3.43 millibarns, where  $k$  is the wave number of the  $\pi^- - p$  system at 960 Mev.

It is then likely that in this state the strange particle production cross section is as great or greater than the  $\pi$  production cross section. However, measurements at higher energies<sup>1</sup> where one might expect more angular momentum states to contribute show that the strange particle production cross section is still small, perhaps 5% of the  $\pi$  production cross section. Cross sections averaged over a wide range of energies tend to approach a fundamental area of interaction. For  $\pi$  mesons this appears to be of the order of the square of the  $\pi$ -meson Compton wavelength. It is plausible that the interaction area for production of strange particles is smaller and of the order of the square of the  $K$ -meson Compton wavelength. If the  $K$  production interaction is quite strong, we would then expect the cross section to rise quickly to about  $(\hbar/M_K c)^2$  and then remain at about this level. The ratio of  $\pi$  to  $K$  production cross sections would be the order of  $(M_K/M_\pi)^2 \approx 12:1$ , a result in accord with the available data.<sup>1,2</sup> Angular distributions measured at higher energies<sup>2</sup> are not inconsistent with this view.<sup>16</sup>

Charge independence imposes certain restrictions upon the relative partial cross sections for the production of  $\Sigma$  particles. If we limit ourselves to any cross section expressible as a square of a single amplitude, we can express this amplitude as the sum of an amplitude  $A_{\frac{1}{2}}$  and an amplitude  $A_{\frac{3}{2}}$ , where the subscript represents the isotopic spin. The cross section,  $\sigma_+$ , for the reaction  $\pi^+ + p = \Sigma^+ + K^+$  will equal  $|A_{\frac{1}{2}}|^2$ ; the cross section,  $\sigma_-$ , for the reaction  $\pi^- + p = \Sigma^- + K^+$  equals  $(1/9)|2A_{\frac{1}{2}} + A_{\frac{3}{2}}|^2$ ; while  $\sigma_0$ , the cross section for the reaction  $\pi^- + p = \Sigma^0 + \theta^0$  equals  $(2/9)|A_{\frac{1}{2}} - A_{\frac{3}{2}}|^2$ . Relationships between the ratios of the cross sections and the ratio and phase differences between the amplitudes are shown in Fig. 6. Since the  $\Sigma$  cross sections at 960 Mev are almost solely due to  $S$ -wave production, it is permissible to use the total cross sections on this diagram. The vertical dashed lines represent the standard error limits of the value  $0.28 \pm 0.10$  for  $(\Sigma^-/\Sigma^0)$  derived from this work multiplied by  $P(\Sigma^0)/P(\Sigma^-)$ , where  $P$  is the center-of-mass momentum. This division of the cross-section ratio by the momentum ratio corrects to a high degree for the difference in thresholds of the two reactions. It would seem unlikely that the

<sup>16</sup> R. K. Adair (to be published).

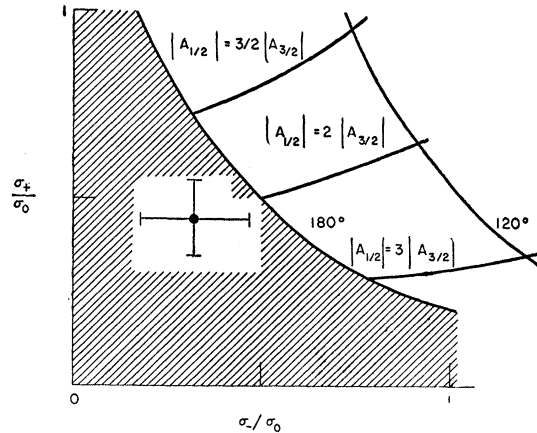


FIG. 6. Ratio of  $\sigma_+$  ( $\Sigma^+ - K^+$ ),  $\sigma_-$  ( $\Sigma^- - K^+$ ) and  $\sigma_0$  ( $\Sigma^0 - \theta^0$ ) from this work and reference 17. Positions of such loci for various ratios and phase differences of the isotopic spin  $\frac{1}{2}$  and  $\frac{3}{2}$  amplitudes are shown. Cross-section ratios in the cross-hatched area violate charge independence.

$\sigma_+$  cross section at 960 Mev would be much greater than the value of  $0.15 \pm 0.04$  millibarn measured at 1.1 Bev by the Michigan group.<sup>17</sup> The horizontal lines of Fig. 6 show this value. These results then suggest a violation of charged independence. Further results of the Michigan Group indicate this more strongly.<sup>18</sup>

Assuming the more likely possibility that our results represent a statistical fluctuation, and that isotopic spin is a good quantum number, we conclude that the ratio of  $(A_{\frac{1}{2}})$  to  $(A_{\frac{3}{2}})$  for  $S$ -wave production of hyperons is about 2:1 and that the amplitudes differ by about  $180^\circ$  in phase.

#### ACKNOWLEDGMENTS

Design and construction of the chamber were greatly facilitated by information informally obtained from other groups. Engineering reports from the University of California Radiation Laboratory, discussions with Professor J. Steinberger, and particularly information from the development work of the Brookhaven Cloud Chamber Group have been very helpful. We are indebted to Mr. C. Theisen and Mr. A. Schlafke of the Brookhaven Engineering department who contributed to the design and development of the chamber, and to Mr. E. Hoyle and Mr. E. Harenberg who were responsible for construction of the chamber. Professor W. F. Hornyak collaborated on early phases of the experiment and Mrs. Gladys Smith and Mrs. Mildred Bracker did much of the scanning.

Much of the success of this work is due to Mr. Richard Larsen who contributed essentially to the design, development, and construction of the chamber, and to operations during the experiment.

<sup>17</sup> Brown, Glaser, Perl, Meyer, Vander Velde, and Cronin, Phys. Rev. **107**, 906 (1957).

<sup>18</sup> J. J. Sakurai, Phys. Rev. **107**, 908 (1957).

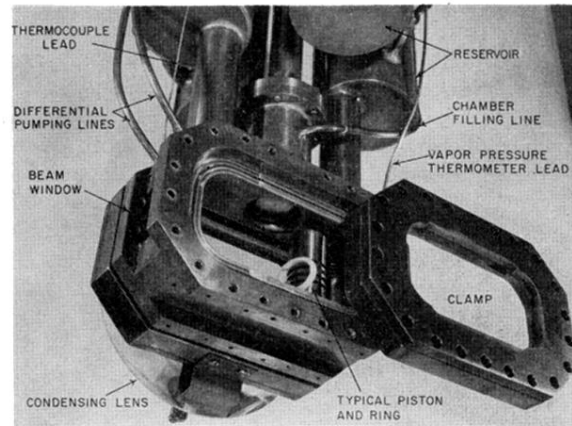


FIG. 1. Schematic view of liquid hydrogen bubble chamber.

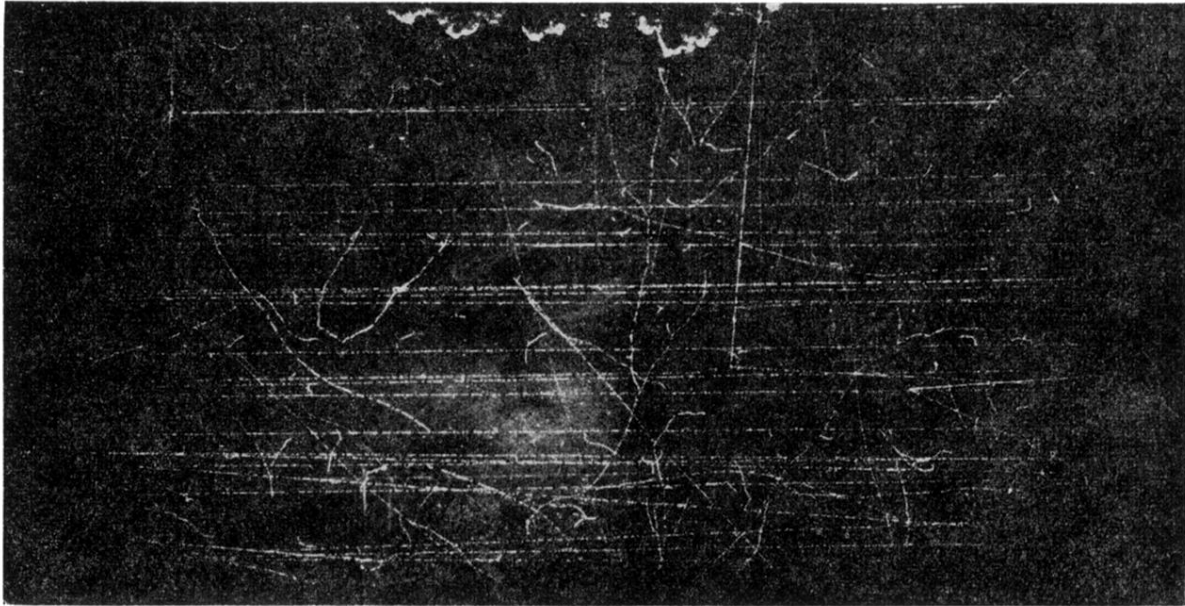


FIG. 2. A  $\pi^- + p \rightarrow \Lambda^0 + \theta^0$  event observed in the bubble chamber.